



Continuous Flow Synthesis of High Valuable N-Heterocycles via Catalytic Conversion of Levulinic Acid

Daily Rodríguez-Padrón¹, Alain R. Puente-Santiago¹, Alina M. Balu¹,
Mario J. Muñoz-Batista^{1*} and Rafael Luque^{1,2*}

¹ Grupo FQM-383, Departamento de Química Orgánica, Universidad de Córdoba, Córdoba, Spain, ² Scientific Center for Molecular Design and Synthesis of Innovative Compounds for the Medical Industry, People's Friendship University of Russia (RUDN University), Moscow, Russia

OPEN ACCESS

Edited by:

Fabio Aricò,
Università Ca' Foscari, Italy

Reviewed by:

Steve Suib,
University of Connecticut,
United States
Svetlana Ivanova,
Universidad de Sevilla, Spain
Christophe Len,
Université de Technologie de
Compiègne, France

*Correspondence:

Mario J. Muñoz-Batista
mq2mubam@uco.es;
jmunoz385x@gmail.com
Rafael Luque
rq62alsor@uco.es

Specialty section:

This article was submitted to
Green and Sustainable Chemistry,
a section of the journal
Frontiers in Chemistry

Received: 09 November 2018

Accepted: 06 February 2019

Published: 26 February 2019

Citation:

Rodríguez-Padrón D,
Puente-Santiago AR, Balu AM,
Muñoz-Batista MJ and Luque R
(2019) Continuous Flow Synthesis of
High Valuable N-Heterocycles via
Catalytic Conversion of Levulinic Acid.
Front. Chem. 7:103.
doi: 10.3389/fchem.2019.00103

Graphitic carbon nitride (g-C₃N₄) was successfully functionalized with a low platinum loading to give rise to an effective and stable catalytic material. The synthesized g-C₃N₄/Pt was fully characterized by XRD, N₂ physisorption, XPS, SEM-Mapping, and TEM techniques. Remarkably, XPS analysis revealed that Pt was in a dominant metallic state. In addition, XPS together with XRD and N₂ physisorption measurements indicated that the g-C₃N₄ preserves its native structure after the platinum deposition process. g-C₃N₄/Pt was applied to the catalytic conversion of levulinic acid to N-heterocycles under continuous flow conditions. Reaction parameters (temperature, pressure, and concentration of levulinic acid) were studied using 3 levels for each parameter, and the best conditions were employed for the analysis of the catalyst's stability. The catalytic system displayed high selectivity to 1-ethyl-5-methylpyrrolidin-2-one and outstanding stability after 3 h of reaction.

Keywords: N-heterocycles, heterogeneous catalysis, graphitic carbon nitride, continuous flow, platinum, Levulinic acid

INTRODUCTION

Biomass has emerged as a competitive alternative for the generation of highly sustainable fuels, chemicals, and drugs (Tuck et al., 2012; Sankaranarayananpillai et al., 2015; Ruppert et al., 2016; Hu et al., 2017; Tang et al., 2017; Filiciotto et al., 2018; Kucherov et al., 2018; Xu W. et al., 2018). A useful strategy for converting biomass feedstocks into fuels and chemicals is based on the transformation of platform molecules, which exhibit high functionality, to form added-value compounds (Serrano-Ruiz et al., 2011; Verma et al., 2017). In this direction, levulinic acid (LA) is a well-known platform molecule that has been widely used toward the fabrication of several valuable compounds such as γ -valerolactone (GVL), which represent a promising fuel source, levulinate esters, which are viable additives for gasoline and diesel transportation fuels, and pyrrolidones, which are involved in industry as surfactants, intermediates for pharmaceuticals, dispersants in fuel additive compositions, solvents and agrochemicals (Huang et al., 2011; Bermudez et al., 2013; Colmenares and Luque, 2014; Touchy et al., 2014; Chatzidimitriou and Bond, 2015; Yan et al., 2015; Ruppert et al., 2016; Gao et al., 2017; Sun et al., 2017; Xu C. et al., 2018).

In the last years, the use of heterogeneous catalysts for the valorization of LA into useful compounds, especially pyrrolidones, has been widely applied (Du et al., 2011; Ogiwara et al., 2016). For instance, the reductive amination of LA with amines in liquid phase has been described using precious metals such as Au, Pd, Pt, Ru, In, and Ir, supported on carbon or metal oxides owing

to their large portfolio of versatile applications (Du et al., 2011; Chatzidimitriou and Bond, 2015; Ogiwara et al., 2016; Zhang et al., 2017). Additionally, a number of endeavors have been made to synthesize novel materials with desirable catalytic properties in order to improve the efficiency of the LA catalytic upgrading toward the production of pyrrolidones (Gao et al., 2017; Sun et al., 2017; Wu et al., 2017). Ultimately, innovative advancements on the design of active and stable heterogeneous catalysts composed of carbon-based materials have been proposed. Zheming Sun et al. have reported a new class of solid molecular N-heterocyclic carbon (NHC) catalysts for the solvent-free reductive amination of biomass-derived levulinic acid to obtain a large variety of interesting structural configurations of *N*-substituted pyrrolidones (Sun et al., 2017). In this regard, NHC-Ru polymer showed high catalytic performance and remarkable reusability, allowing the development of one-pot tandem reductive reactions of LA with aldehydes or ketones.

Graphitic carbon nitride, generally known as $g\text{-C}_3\text{N}_4$, is recognized as the most stable allotrope among various carbon nitrides under ambient conditions. The surface chemistry of its polymeric structure can be easily controlled via molecular-level modification and surface engineering. Additionally, the polymeric nature of $g\text{-C}_3\text{N}_4$ guarantees sufficient flexibility of the structure, which can serve as a compatible matrix for the anchorage of various inorganic nanoparticles and consequently can be successfully applied in a myriad of photocatalytic applications (Muñoz-Batista et al., 2015b, 2016, 2018; Xue et al., 2015; Fontelles-Carceller et al., 2016; Sastre et al., 2016; Zeng et al., 2017; Hak et al., 2018; Majeed et al., 2018). Despite the mentioned applications, graphitic carbon nitride-based materials have not been broadly employed toward the catalytic valorization of biomass-derived chemicals. A representative example in which an organic sulfonated graphitic carbon nitride was used for conversion of carbohydrates into furanics and related value-added products can be highlighted (Verma et al., 2017).

We report herein the reductive amination of levulinic acid into highly valuable pyrrolidones driven by $g\text{-C}_3\text{N}_4/\text{Pt}$ composites as a competitive catalyst. The catalytic processes were performed under flow conditions which ensure high control over reaction conditions, fast and effective reagent mixing and shorter times of reactions (Bermudez et al., 2013; Chen et al., 2015; Gemoets et al., 2016; Muñoz-Batista et al., 2018).

EXPERIMENTAL

Materials

All chemicals were obtained from Sigma-Aldrich with pure analytical degree.

Synthesis of $g\text{-C}_3\text{N}_4/\text{Pt}$ Composites

The graphitic carbon nitride was obtained by calcination of melamine in a semi-closed system at 580°C for 4 h using a heating rate of 5°C min^{-1} . In order to improve its superficial area, the obtained bulk $g\text{-C}_3\text{N}_4$ was treated by ultrasonication for 5 h in deionized water using 1 mg mL^{-1} . The platinum component was deposited using a simple chemical reduction method. The $g\text{-C}_3\text{N}_4$ support was suspended by stirring in

deionized water solution for 30 min. Then, the proper quantity of H_2PtCl_6 was added to the solution to get 1 wt.% of Pt on metal basis and kept under stirring for 15 min. Finally, a hydrazine aqueous solution was quickly added, where the molar ratio between Pt and hydrazine was fixed to 1:5. The resulting mixture was stirred for 30 min and separated by filtration. The separated solid was rinsed with distilled water and dried at 80°C for 16 h. The Pt loading in the sample was 1 wt.%, confirmed by ICP-MS analysis in an Elan DRC-e (PerkinElmer SCIEX) spectrometer.

Catalyst Characterization

XRD experiments were performed in the Bruker D8 Advance Diffractometer with the LynxEye detector. The XRD patterns were recorded in a 2θ scan range from 10 to 80° . Phase identification was carried out using Bruker Diffrac-plus Eva software, supported by the Power Diffraction File Database. N_2 physisorption experiments were accomplished with the Micromeritics ASAP 2000 instrument. The sample was previously degassed for 24 h under vacuum ($p < 10^{-2}$ Pa). Moreover, TEM images were recorded in the JEOL JEM 1400 instrument and assembled with a charge-coupling camera device. Samples were previously suspended in ethanol and deposited on a copper grid. SEM-EDX micrographs were acquired in the JEOL-SEM JSM-7800 LV scanning microscope. XPS measurements were accomplished with an ultrahigh vacuum multipurpose surface analysis instrument, SpecsTM. Prior to the analysis, the sample was evacuated overnight under vacuum (10^{-6} Torr). XPS spectra were acquired at room temperature using a conventional X-ray source with a Phoibos 150-MCD energy detector. XPS CASA software was employed to analyze the obtained results.

Catalytic Experiments

Catalytic performance of the obtained catalytic materials was evaluated in the H-Cube Mini PlusTM flow hydrogenation

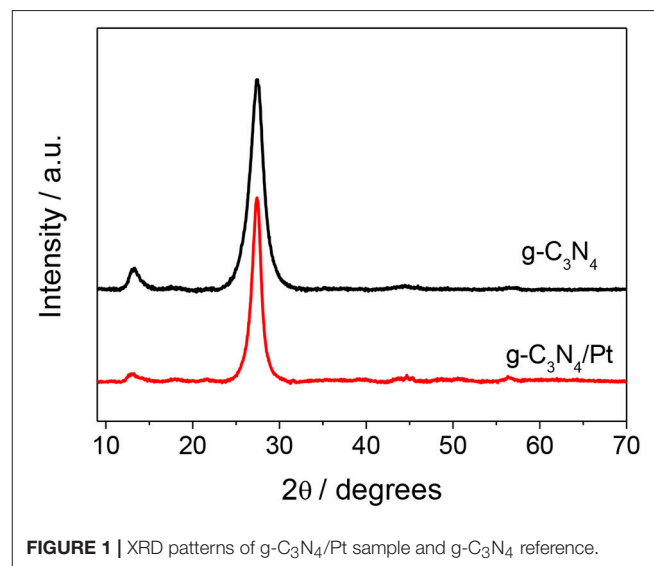


FIGURE 1 | XRD patterns of $g\text{-C}_3\text{N}_4/\text{Pt}$ sample and $g\text{-C}_3\text{N}_4$ reference.

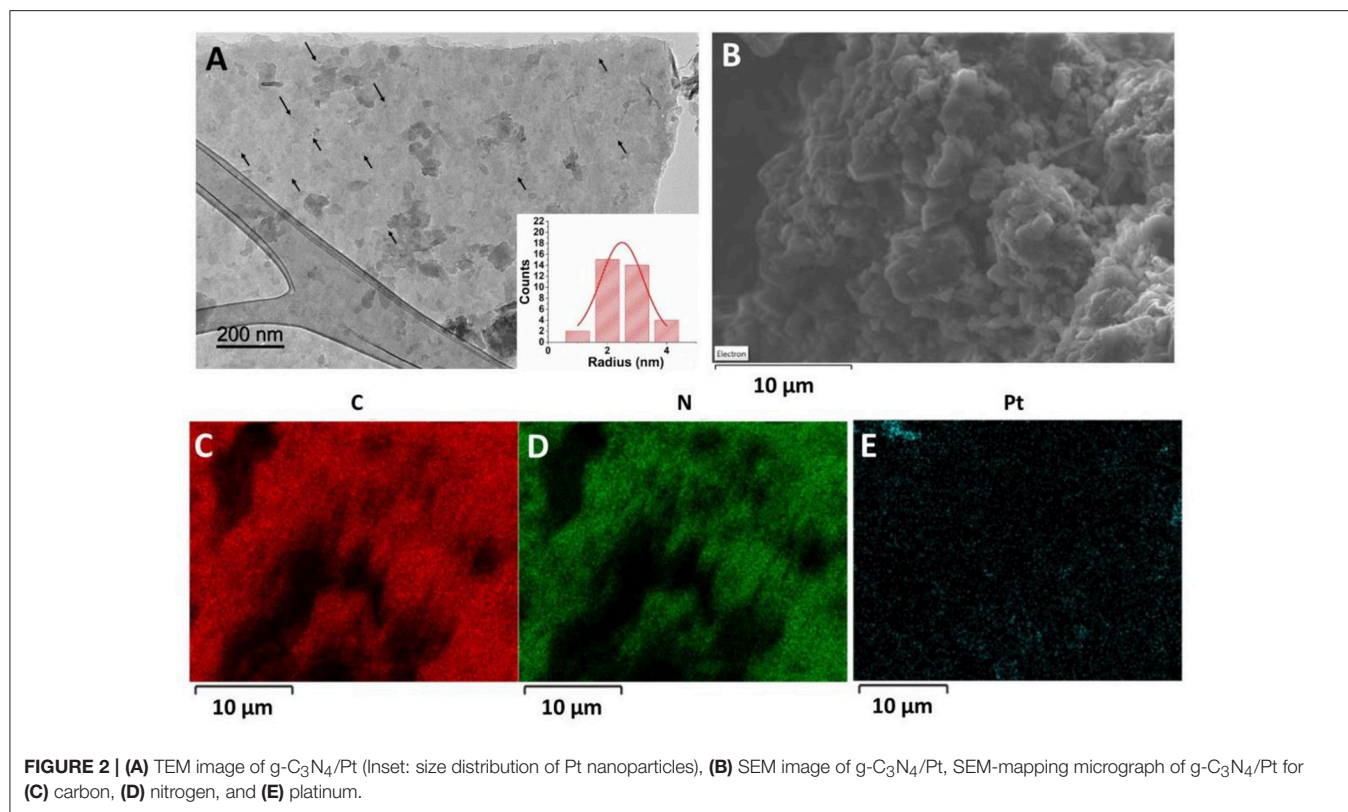


TABLE 1 | Morphological properties of g-C₃N₄/Pt sample and g-C₃N₄ reference.

Sample	BET surface area (m ² g ⁻¹)	Pore volume (cm ³ g ⁻¹)	Pore size (nm)	Pt particle size (nm)
g-C ₃ N ₄	58	0.2	15.7	–
g-C ₃ N ₄ /Pt	54	0.2	15.8	2.5

reactor. The catalysts were packed (ca. 0.1 g of catalyst per cartridge) in 30 mm-long ThalesNano CatCarts. The system was firstly washed with (1) methanol and (2) acetonitrile (0.3 mL/min, 20 min for each solvent). A solution of levulinic acid in acetonitrile was subsequently pumped through and the reaction conditions were set. The required hydrogen was generated *in situ* during the reaction by water electrolysis in the H-Cube equipment. The reactions were followed for 120 min, where a stationary situation was reached, and the collected samples were analyzed by GC-MS.

The conversion, selectivity and stability achieved for the catalyst in the reaction were investigated by gas chromatography (GC) in an Agilent 6890N gas chromatograph (60 mL min⁻¹ N₂ carrier flow, 20 psi column top head pressure) using a flame ionization detector (FID). The capillary column HP-5 (30 m × 0.32 mm × 0.25 mm) was employed. In addition, the collected liquid fractions were analyzed by GC-MS—using the Agilent 7820A GC/5977B High Efficiency Source (HES) MSD—in order to identify the obtained products.

RESULTS AND DISCUSSION

X-ray diffraction analysis was employed to identify the structure and arrangement of the synthesized graphitic carbon nitride as well as the platinum-modified sample. As shown in **Figure 1**, both samples presented the typical interlayer-stacking (002) reflection of disordered carbon in a graphitic g-C₃N₄ layered structure and a peak around 13.1°, associated to the (100) reflection (Muñoz-Batista et al., 2016). The position of the (002) plane also showed the typical shift (~0.3), in comparison with the bulk counterpart, which can be related to the decrease of the interlayer distance, which takes place during the ultrasonication process (Muñoz-Batista et al., 2017). As has been analyzed in previous reports, the limitation of the number of sheets stacked produces the weakening of interlayer forces with effect in the corrugation of the layers and the subsequent decrease of the corresponding distance between layers (Niu et al., 2012; Muñoz-Batista et al., 2017). The XRD pattern of g-C₃N₄/Pt has not displayed considerable changes in comparison with the unmodified material and therefore did not offer information about the Pt phases, most likely due to the relatively limited amount of the noble metal in the final material.

Morphology of the synthesized g-C₃N₄/Pt was studied by microscopy (TEM and SEM) analyses (**Figure 2**). g-C₃N₄/Pt exhibited a laminar structure, as can be observed in **Figure 2A**. TEM analyses also allowed the identification of small platinum nanoparticles with a mean diameter of 2.5 nm on the g-C₃N₄/Pt surface (**Table 1**). Importantly,

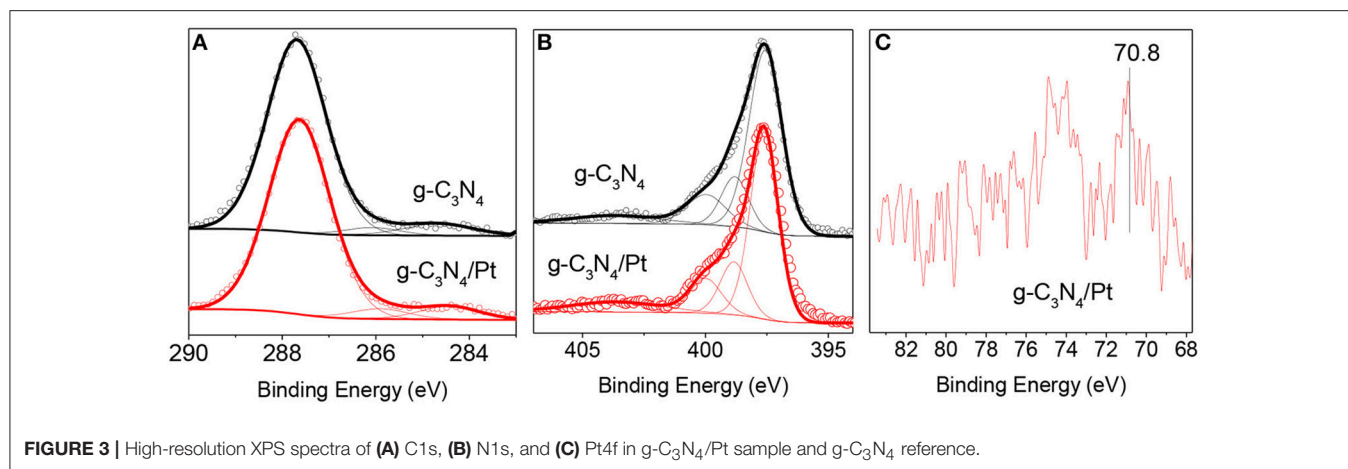


FIGURE 3 | High-resolution XPS spectra of (A) C1s, (B) N1s, and (C) Pt4f in g-C₃N₄/Pt sample and g-C₃N₄ reference.

TABLE 2 | C1s and N1s XPS region fitting results of g-C₃N₄ and g-C₃N₄/Pt.

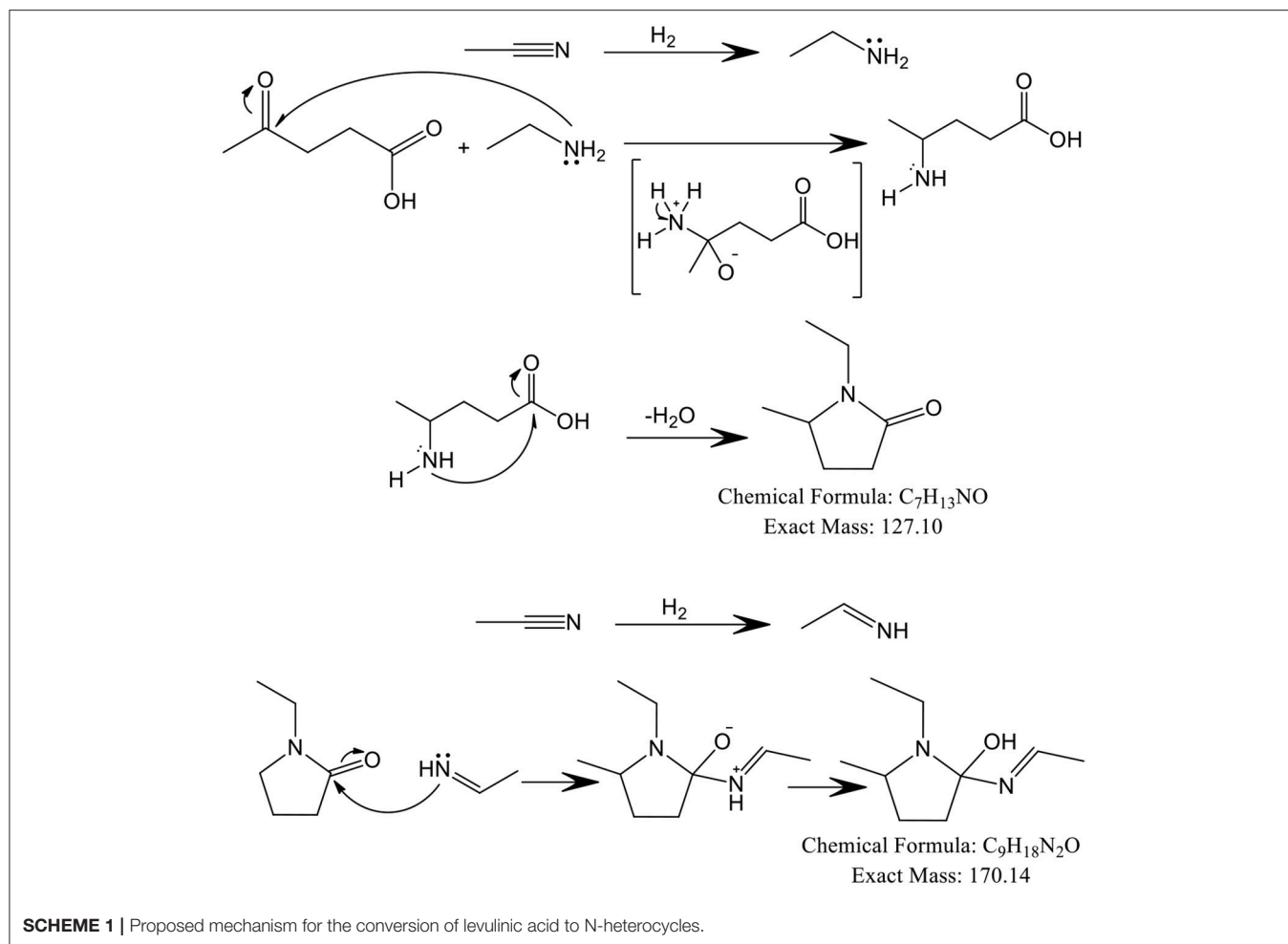
N1s								
Sample	C-N-C	%	(C)3-N	%	N-H	%	Pi-exc.	%
g-C ₃ N ₄	397.5	58.5	399.2	24	400.5	12	403.4	5.5
g-C ₃ N ₄ /Pt	397.2	58	399.0	24	400.4	12.5	403.6	5.5
C1s								
Sample	C-C	%	(C)3-N	%	C-N-C	%		
g-C ₃ N ₄	284.6	8	286.2	5	287.6	87		
g-C ₃ N ₄ /Pt	284.6	9	286.2	5.5	287.5	85.5		

EDX-mapping micrographs of g-C₃N₄/Pt also confirmed the successful functionalization of graphitic carbon nitride with platinum, which depicts a relative homogeneous distribution. As is summarized in **Table 1**, the Pt-modified material showed rather similar values to the pure g-C₃N₄ reference in all the parameters determined by N₂ physisorption (BET Surface area, pore volume, pore size). BET surface area above 50 m² g⁻¹ and a dominant mesoporous structure could be originated from the void volume created by the agglomeration of the g-C₃N₄ sheets, allowing an efficient deposition of the metallic entities (**Table 1**).

The structural analysis of g-C₃N₄/Pt and g-C₃N₄ was completed with the help of X-ray photoelectron spectroscopy. XPS measurements were carried out in order to provide information related to the carbon, nitrogen, and platinum components. **Figure 3** shows the XPS spectra for the two catalytic systems, including C1s (**Figure 3A**), N1s (**Figure 3B**), and Pt4f (**Figure 3C**) regions. The summary of the N- and C-containing species contributing to the C1s and N1s peaks of the sample and g-C₃N₄ reference is presented in **Table 2**. The C1s XPS region showed contributions from C₃-N (~286.2 eV), N-C-N (~287.6 eV) and C-C (~284.6 eV) (Muñoz-Batista et al., 2015a). C₃-N and N-C-N can be exclusively ascribable to g-C₃N₄ while C-C contribution, which was also used as reference, energy can be associated with surface residues or defects in the nanopolymer structure (Wanger et al., 1979). For the N1s XPS region, besides C₃-N (~399.1 eV) and N-C-N (~397.5 eV), two more

contributions were used during the deconvolution procedure; N-H (~400.4 eV) and the typical broad pi-exc (~403.5 eV) (Muñoz-Batista et al., 2015a). In conclusion, **Figures 3A,B** as well as the data of **Table 2** provide evidence of the strong similitude detected between the pure g-C₃N₄ and Pt/g-C₃N₄ samples. XPS also allowed the detection of minority components in the structure, namely Pt nanoparticles. Although the signal-to-noise ratio of the Pt XPS region (**Figure 3C**) is relatively low, the shape of the Pt4f is indicative of a dominant metallic state (~71 eV) (Fontelles-Carceller et al., 2017).

The catalytic performance of the prepared materials was evaluated in the conversion of levulinic acid to nitrogen-heterocycles under continuous flow conditions. N-heterocycles were obtained via condensation of levulinic acid, an 1,4-dicarbonyl compound, with an excess of ethylamine (**Scheme 1**) (Li, 2014). In this case, acetonitrile acts both as solvent and reactant, giving rise to ethylamine by *in situ* hydrogenation. The cyclization step involves a nucleophilic addition on a carbonyl group by the nitrogen of an intermediate. Levulinic acid acts as an electrophile both in the initial step of the reaction with the amine and in the cyclization step. After formation of the cyclic compound, the reaction proceeded via alcohol dehydration to produce the corresponding alkene. The hydroxyl (OH) group donates two electrons to H⁺, generating an alkylloxonium ion, which can act as a good leaving group. The formed alkene is effectively hydrogenated under hydrogen pressure to give rise to 1-ethyl-5-methylpyrrolidin-2-one, C₇H₁₃NO (127.10 g/mol).

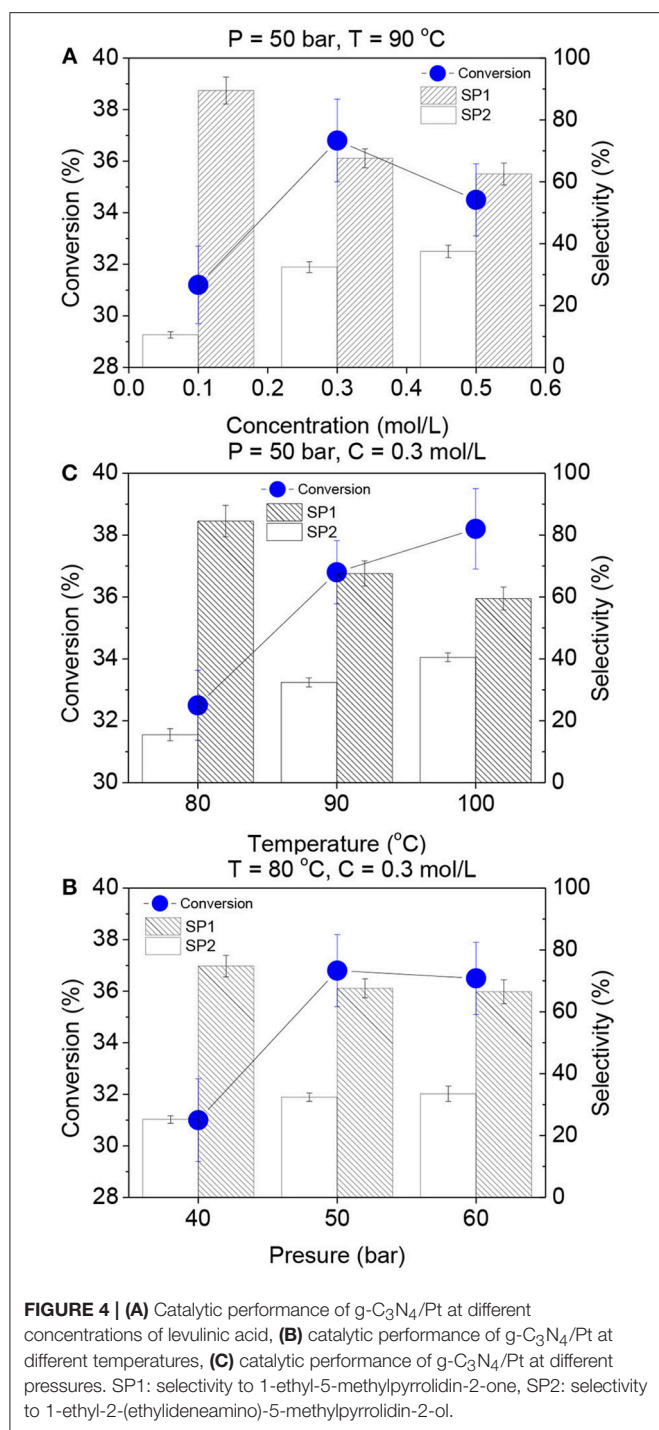


In addition, the formation of 1-ethyl-2-(ethylideneamino)-5-methylpyrrolidin-2-ol, $C_9H_{18}N_2O$ (170.14 g/mol) can be understood if we take into account that hydrogenation of acetonitrile did not just give rise to ethylamine but also to ethanimine, which can further attack the carbonyl group of 1-ethyl-5-methylpyrrolidin-2-one with the consequential formation of 1-ethyl-2-(ethylideneamino)-5-methylpyrrolidin-2-ol.

Firstly, a complete parametric analysis was accomplished in order to optimize the reaction conditions. In this regard, three levels of temperature, pressure and concentration were explored in the reaction of levulinic acid to N-heterocycles for 120 min (**Figure 4**). Carbon balance was achieved above 97% in all catalytic tests. Influence of the concentration in conversion and selectivity values was unraveled, as shown in **Figure 4A**. 0.3 mol/L was selected as the optimum concentration for the employed catalytic system. Although a lower concentration (0.1 mol/L) resulted in higher selectivity to 1-ethyl-5-methylpyrrolidin-2-one and the 0.5 mol/L concentration showed similar selectivity values, 0.3 mol/L gave rise to the best balance between conversion and selectivity.

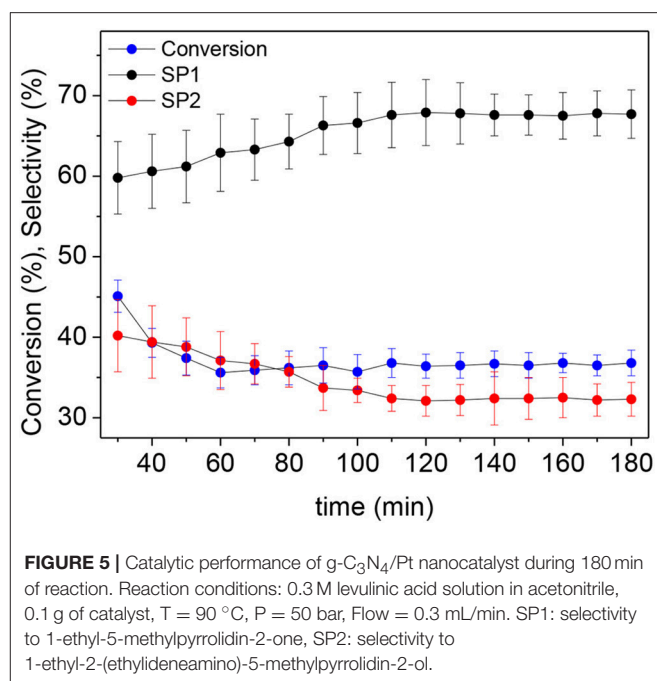
The effect of temperature in the catalytic performance has been investigated by performing the reaction at 80, 90, and 100°C (**Figure 4B**). Additionally, influence of the system pressure was evaluated by accomplishing the reaction at 40, 50, and 60 bars (**Figure 4C**). In both cases an increment of the conversion and a decrease of the selectivity (1-ethyl-5-methylpyrrolidin-2-one) was observed for higher pressure and temperature values. Although 60 bars and 100°C conditions showed similar catalytic performance, 50 bars and 90°C were selected as the optimum pressure and temperature due to the good balance in conversion and selectivity, avoiding higher energy consumption reaction parameters. In addition, blank measurements were performed without a catalyst or employing $g-C_3N_4$, revealing that the reaction does not proceed in absence of an effective catalytic system.

Once the reaction parameters were optimized, the stability of the prepared catalytic system was investigated by performing the reaction for 3 h. After obtaining a stationary state (typically obtained after 120 min of reaction), a conversion of 36.8% employing $g-C_3N_4/Pt$ was achieved. **Figure 5** shows details of the flow catalytic process in terms of conversion and selectivity. The



performed reaction gave rise to 1-ethyl-2-(ethylideneamino)-5-methylpyrrolidin-2-ol, $\text{C}_9\text{H}_{18}\text{N}_2\text{O}$ (170.14 g/mol), and 1-ethyl-5-methylpyrrolidin-2-one, $\text{C}_7\text{H}_{13}\text{NO}$ (127.10 g/mol), with the last being the major product (67.6% of selectivity). Remarkably, the catalytic system displayed outstanding stability without considerable loss of activity for up to 3 h of reaction.

The structure of both products was proposed considering the fragmentation pattern in the MS spectra (Figure S1). The



aforementioned compounds have a common fragmentation pattern and therefore a common skeleton. The molecular ions of $\text{C}_7\text{H}_{13}\text{NO}$ and $\text{C}_9\text{H}_{18}\text{N}_2\text{O}$ were found at m/z 127.1 and 169.1, respectively.

CONCLUSIONS

In summary, this contribution has aimed to explore a strategy for biomass valorization through the catalytic conversion of levulinic acid, a platform molecule, to N-heterocycles. A simple procedure has been applied for the synthesis of an active, effective and stable catalytic system with a low noble-metal concentration ($g\text{-C}_3\text{N}_4/\text{Pt}$). The catalytic performance of the aforementioned material was investigated in the continuous flow transformation of levulinic acid to valuable N-heterocycles. A complete parametric analysis was performed by changing the reaction conditions, namely temperature, pressure and concentration of levulinic acid. The optimum balance between conversion and selectivity was found by using 3 M levulinic acid solution in acetonitrile at $T = 90^\circ\text{C}$ and $P = 50$ bars. Remarkably, the catalyst was highly selective (67.5%) to the formation of 1-ethyl-5-methylpyrrolidin-2-one and exceptionally stable during 3 h of reaction.

AUTHOR CONTRIBUTIONS

DR-P performed all experiments and wrote the first draft of the manuscript. AP-S supported the experimental work and revised the manuscript draft. AB finalized the draft with RL, conceived the experimental work and provided lab and financial support. MM-B conceived and planned the experiments with RL and finished the manuscript for submission. RL provided the lab for

all experiments, planned the experimental work, and finalized and submitted the manuscript.

ACKNOWLEDGMENTS

RL gratefully acknowledges support from MINECO under project CTQ2016-78289-P, co-financed with FEDER funds. Both DR-P and AP-S also gratefully acknowledge MINECO for providing research contracts under the same project. MM-B

REFERENCES

- Bermudez, J. M., Menéndez, J. A., Romero, A. A., Serrano, E., Garcia-Martinez, J., and Luque, R. (2013). Continuous flow nanocatalysis: reaction pathways in the conversion of levulinic acid to valuable chemicals. *Green Chem.* 15, 2786–2792. doi: 10.1039/c3gc41022f
- Chatzidimitriou, A., and Bond, J. Q. (2015). Oxidation of levulinic acid for the production of maleic anhydride: breathing new life into biochemicals. *Green Chem.* 17, 4367–4376. doi: 10.1039/C5GC01000D
- Chen, M., Ichikawa, S., and Buchwald, S. L. (2015). Rapid and efficient copper-catalyzed finkelstein reaction of (hetero)aromatics under continuous-flow conditions. *Angew. Chem. Int. Ed.* 54, 263–266. doi: 10.1002/anie.201409595
- Colmenares, J. C., and Luque, R. (2014). Heterogeneous photocatalytic nanomaterials: prospects and challenges in selective transformations of biomass-derived compounds. *Chem. Soc. Rev.* 43, 765–778. doi: 10.1039/C3CS60262A
- Du, X.-L., He, L., Zhao, S., Liu, Y.-M., Cao, Y., He, H.-Y., et al. (2011). Hydrogen-independent reductive transformation of carbohydrate biomass into γ -valerolactone and pyrrolidone derivatives with supported gold catalysts. *Angew. Chemie* 123, 7961–7965. doi: 10.1002/ange.201100102
- Filiciotto, L., Balu, A. M., Van der Waal, J. C., and Luque, R. (2018). Catalytic insights into the production of biomass-derived side products methyl levulinate, furfural and humins. *Catal. Today* 302, 2–15. doi: 10.1016/j.cattod.2017.03.008
- Fontelles-Carceller, O., Muñoz-Batista, M. J., Fernández-García, M., and Kubacka, A. (2016). Interface effects in sunlight-driven Ag/g-C₃N₄ composite catalysts: study of the toluene photodegradation quantum efficiency. *ACS Appl. Mater. Interfaces* 8, 2617–2627. doi: 10.1021/acsami.5b10434
- Fontelles-Carceller, O., Muñoz-Batista, M. J., Rodríguez-Castellón, E., Conesa, J. C., Fernández-García, M., and Kubacka, A. (2017). Measuring and interpreting quantum efficiency for hydrogen photo-production using Pt-titanania catalysts. *J. Catal.* 347, 157–169. doi: 10.1016/j.jcat.2017.01.012
- Gao, G., Sun, P., Li, Y., Wang, F., Zhao, Z., Qin, Y., et al. (2017). Highly stable porous-carbon-coated ni catalysts for the reductive amination of levulinic acid via an unconventional pathway. *ACS Catal.* 7, 4927–4935. doi: 10.1021/acscatal.7b01786
- Gemoets, H. P. L., Su, Y., Shang, M., Hessel, V., Luque, R., and Noël, T. (2016). Liquid phase oxidation chemistry in continuous-flow microreactors. *Chem. Soc. Rev.* 45, 83–117. doi: 10.1039/C5CS00447K
- Hak, C. H., Sim, L. C., Leong, K. H., Lim, P. F., Chin, Y. H., and Saravanan, P. (2018). M/g-C₃N₄ (M=Ag, Au, and Pd) composite: synthesis via sunlight photodeposition and application towards the degradation of bisphenol A. *Environ. Sci. Pollut. Res.* 25, 25401–25412. doi: 10.1007/s11356-018-2632-8
- Hu, L., Lin, L., Wu, Z., Zhou, S., and Liu, S. (2017). Recent advances in catalytic transformation of biomass-derived 5-hydroxymethylfurfural into the innovative fuels and chemicals. *Renew. Sustain. Energy Rev.* 74, 230–257. doi: 10.1016/j.rser.2017.02.042
- Huang, Y. B., Dai, J. J., Deng, X. J., Qu, Y. C., Guo, Q. X., and Fu, Y. (2011). Ruthenium-catalyzed conversion of levulinic acid to pyrrolidines by reductive amination. *ChemSusChem* 4, 1578–1581. doi: 10.1002/cssc.201100344
- Kucherov, F. A., Romashov, L. V., Galkin, K. I., and Ananikov, V. P. (2018). Chemical transformations of biomass-derived C6-furanic platform chemicals for sustainable energy research, materials science, and synthetic building blocks. *ACS Sustain. Chem. Eng.* 6, 8064–8092. doi: 10.1021/acssuschemeng.8b00971
- Li, J. J. (ed.). (2014). “Paal–Knorr pyrrole synthesis,” in *Name Reactions* (Cham: Springer International Publishing), 454–455. doi: 10.1007/978-3-319-03979-4_202
- Majeed, I., Manzoor, U., Kanodarwala, F. K., Nadeem, M. A., Hussain, E., Ali, H., et al. (2018). Pd–Ag decorated g-C₃N₄ as an efficient photocatalyst for hydrogen production from water under direct solar light irradiation. *Catal. Sci. Technol.* 8, 1183–1193. doi: 10.1039/C7CY02219K
- Muñoz-Batista, M. J., Fernández-García, M., and Kubacka, A. (2015a). Promotion of CeO₂–TiO₂ photoactivity by g-C₃N₄: ultraviolet and visible light elimination of toluene. *Appl. Catal. B Environ.* 164, 261–270. doi: 10.1016/j.apcatb.2014.09.037
- Muñoz-Batista, M. J., Fontelles-Carceller, O., Ferrer, M., Fernández-García, M., and Kubacka, A. (2016). Disinfection capability of Ag/g-C₃N₄ composite photocatalysts under UV and visible light illumination. *Appl. Catal. B Environ.* 183, 86–95. doi: 10.1016/j.apcatb.2015.10.024
- Muñoz-Batista, M. J., Fontelles-Carceller, O., Kubacka, A., and Fernández-García, M. (2017). Effect of exfoliation and surface deposition of MnOx species in g-C₃N₄: toluene photo-degradation under UV and visible light. *Appl. Catal. B Environ.* 203, 663–672. doi: 10.1016/j.apcatb.2016.10.044
- Muñoz-Batista, M. J., Nasalevich, M. A., Savenije, T. J., Kapteijn, F., Gascon, J., Kubacka, A., et al. (2015b). Enhancing promoting effects in g-C₃N₄-Mⁿ⁺/CeO₂-TiO₂ ternary composites: photo-handling of charge carriers. *Appl. Catal. B Environ.* 176–177, 687–698. doi: 10.1016/j.apcatb.2015.04.051
- Muñoz-Batista, M. J., Rodríguez-Padrón, D., Puente-Santiago, A. R., Kubacka, A., Luque, R., and Fernández-García, M. (2018). Sunlight-driven hydrogen production using an annular flow photoreactor and g-C₃N₄-based catalysts. *ChemPhotoChem* 2, 870–977. doi: 10.1002/cptc.201800064
- Niu, P., Zhang, L., Liu, G., and Cheng, H.-M. (2012). Graphene-like carbon nitride nanosheets for improved photocatalytic activities. *Adv. Funct. Mater.* 22, 4763–4770. doi: 10.1002/adfm.201200922
- Ogiwara, Y., Uchiyama, T., and Sakai, N. (2016). Reductive amination/cyclization of keto acids using a hydrosilane for selective production of lactams versus cyclic amines by switching of the indium catalyst. *Angew. Chemie* 128, 1896–1899. doi: 10.1002/ange.201509465
- Ruppert, A. M., Jedrzejczyk, M., Sneka-Platek, O., Keller, N., Dumon, A. S., Michel, C., et al. (2016). Ru catalysts for levulinic acid hydrogenation with formic acid as a hydrogen source. *Green Chem.* 18, 2014–2028. doi: 10.1039/C5GC02200B
- Sankaranarayananpillai, S., Sreekumar, S., Gomes, J., Grippo, A., Arab, G. E., Head-Gordon, M., et al. (2015). Catalytic upgrading of biomass-derived methyl ketones to liquid transportation fuel precursors by an organocatalytic approach. *Angew. Chemie Int. Ed.* 54, 4673–4677. doi: 10.1002/anie.201412470
- Sastre, F., Muñoz-Batista, M. J., Kubacka, A., Fernández-García, M., Smith, W. A., Kapteijn, F., et al. (2016). Efficient electrochemical production of syngas from CO₂ and H₂O by using a Nanostructured Ag/g-C₃N₄ Catalyst. *ChemElectroChem* 3, 1497–1502. doi: 10.1002/celec.201600392
- Serrano-Ruiz, J. C., Luque, R., and Sepúlveda-Escribano, A. (2011). Transformations of biomass-derived platform molecules: from high added-value chemicals to fuels via aqueous-phase processing. *Chem. Soc. Rev.* 40:5266. doi: 10.1039/c1cs15131b
- Sun, Z., Chen, J., and Tu, T. (2017). NHC-based coordination polymers as solid molecular catalysts for reductive amination of biomass levulinic acid. *Green Chem.* 19, 789–794. doi: 10.1039/C6GC02591A

- Tang, X., Wei, J., Ding, N., Sun, Y., Zeng, X., Hu, L., et al. (2017). Chemoselective hydrogenation of biomass derived 5-hydroxymethylfurfural to diols: key intermediates for sustainable chemicals, materials and fuels. *Renew. Sustain. Energy Rev.* 77, 287–296. doi: 10.1016/J.RSER.2017.04.013
- Touchy, A. S., Hakim Siddiki, S. M. A., Kon, K., and Shimizu, K. (2014). Heterogeneous Pt Catalysts for reductive amination of levulinic acid to pyrrolidones. *ACS Catal.* 4, 3045–3050. doi: 10.1021/cs500757k
- Tuck, C. O., Pérez, E., Horváth, I. T., Sheldon, R. A., and Poliakoff, M. (2012). Valorization of biomass: deriving more value from waste. *Science* 337, 695–699. doi: 10.1126/science.1218930
- Verma, S., Baig, R. B. N., Nadagouda, M. N., Len, C., and Varma, R. S. (2017). Sustainable pathway to furanics from biomass via heterogeneous organo-catalysis. *Green Chem.* 19, 164–168. doi: 10.1039/C6GC02551J
- Wanger, C. D., Riggs, W. M., Davis, L. E., Moulder, J. F., and Muilenberg, E. G. (1979). *Handbook of X-Ray Photoelectron Spectroscopy: A Reference Book of Standard Data for Use in X-Ray Photoelectron Spectroscopy*. Eden Prairie, MN: Physical Electronics Division, Perkin-Elmer Corp.
- Wu, C., Zhang, H., Yu, B., Chen, Y., Ke, Z., Guo, S., et al. (2017). Lactate-based ionic liquid catalyzed reductive amination/cyclization of keto acids under mild conditions: a metal-free route to synthesize lactams. *ACS Catal.* 7, 7772–7776. doi: 10.1021/acscatal.7b02231
- Xu, C., Ouyang, W., Munoz-Batista, M. J., Fernandez-Garcia, M., and Luque, R. (2018). Highly active catalytic Ru/TiO₂ nanomaterials for continuous flow production of γ -valerolactone. *ChemSusChem* 11, 2604–2611. doi: 10.1002/cssc.201800667
- Xu, W., Wang, X., Sandler, N., Willför, S., and Xu, C. (2018). Three-dimensional printing of wood-derived biopolymers: a review focused on biomedical applications. *ACS Sustain. Chem. Eng.* 6, 5663–5680. doi: 10.1021/acssuschemeng.7b03924
- Xue, J., Ma, S., Zhou, Y., Zhang, Z., and He, M. (2015). Facile photochemical synthesis of Au/Pt/g-C₃N₄ with plasmon-enhanced photocatalytic activity for antibiotic degradation. *ACS Appl. Mater. Interfaces* 7, 9630–9637. doi: 10.1021/acsami.5b01212
- Yan, K., Jarvis, C., Gu, J., and Yan, Y. (2015). Production and catalytic transformation of levulinic acid: a platform for speciality chemicals and fuels. *Renew. Sustain. Energy Rev.* 51, 986–997. doi: 10.1016/J.RSER.2015.07.021
- Zeng, Z., Li, K., Wei, K., Dai, Y., Yan, L., Guo, H., et al. (2017). Fabrication of highly dispersed platinum-deposited porous g-C₃N₄ by a simple *in situ* photoreduction strategy and their excellent visible light photocatalytic activity toward aqueous 4-fluorophenol degradation. *Chinese J. Catal.* 38, 29–38. doi: 10.1016/S1872-2067(16)62589-5
- Zhang, J., Xie, B., Wang, L., Yi, X., Wang, C., Wang, G., et al. (2017). Zirconium oxide supported palladium nanoparticles as a highly efficient catalyst in the hydrogenation-amination of levulinic acid to pyrrolidones. *ChemCatChem* 9, 2661–2667. doi: 10.1002/cctc.201600739

Conflict of Interest Statement: The authors declare that the research was conducted in the absence of any commercial or financial relationships that could be construed as a potential conflict of interest.

The reviewer CL declared a past co-authorship with one of the authors RL to the handling editor.

Copyright © 2019 Rodríguez-Padrón, Puente-Santiago, Balu, Muñoz-Batista and Luque. This is an open-access article distributed under the terms of the Creative Commons Attribution License (CC BY). The use, distribution or reproduction in other forums is permitted, provided the original author(s) and the copyright owner(s) are credited and that the original publication in this journal is cited, in accordance with accepted academic practice. No use, distribution or reproduction is permitted which does not comply with these terms.